CD271 Down-Regulation Promotes Melanoma Progression and Invasion in Three-Dimensional Models and in Zebrafish

Annalisa Saltari[1,4], Francesca Truzzi[1,4], Marika Quadri[1], Roberta Lotti[1], Elisabetta Palazzo[1], Giulia Grisendi[2], Natascia Tiso[3], Alessandra Marconi[1] and Carlo Pincelli[1]

CD271 is a neurotrophin receptor variably expressed in melanoma. Although contradictory data are reported on its role as a marker of tumor-initiating cells, little is known about its function in tumor progression. CD271 expression was higher in spheroids derived from freshly isolated cells of primary melanomas and in primary WM115 and WM793-B cell lines, and it decreased during progression to advanced stages in cells isolated from metastatic melanomas and in metastatic WM266-4 and 1205Lu cell lines. Moreover, CD271 was scarcely detected in the highly invasive spheroids (SKMEL28 and 1205Lu). CD271, originally expressed in the epidermis of skin reconstructs, disappeared when melanoma started to invade the dermis. SKMEL8 CD271$^-$ cells showed greater proliferation and invasiveness in vitro and were associated with a higher number of metastases in zebrafish compared with CD271$^+$ cells. CD271 silencing in WM115 induced a more aggressive phenotype in vitro and in vivo. On the contrary, CD271 overexpression in SKMEL28 cells reduced invasion in vitro, and CD271 overexpressing 1205Lu cells was associated with a lower percentage of metastases in zebrafish. A reduced cell-cell adhesion was also observed in the absence of CD271. Taken together, these results indicate that CD271 loss is critical for melanoma progression and metastasis.

Journal of Investigative Dermatology (2016) **136,** 2049–2058; doi:10.1016/j.jid.2016.05.116

INTRODUCTION

Melanoma is the deadliest type of skin cancer, and its incidence is rising faster than that of any other solid tumor (Eggermont et al., 2014). Although early melanomas can be cured by surgical excision, metastatic melanomas are generally fatal because of their resistance to current chemotherapies (Gray-Shopfer et al., 2007) Melanoma arises from a precursor, enters the radial growth phase with cells proliferating in the epidermis, invades the dermis, and starts the vertical growth phase. We have previously shown that melanoma cells express neurotrophins and their receptors and play a role in tumor progression (Truzzi et al., 2008). Neurotrophins bind two classes of receptors: the high-affinity receptors (Trks) and the low-affinity receptor (p75^{NTR} or CD271). CD271 was first isolated from a melanoma cell line and is expressed on neural crest cells, from which melanocytes are derived (Kruger et al., 2002). It belongs to the tumor necrosis factor receptor superfamily and mediates apoptosis in different cell settings via its own signaling pathway (Blöchl and Blöch, 2007; Kraemer et al., 2014; Truzzi et al., 2011). The interaction of apoptosis-related protein (APR)-1 with CD271 activates apoptosis in melanoma cells (Selimovic et al., 2012). CD271 activation mediates apoptosis in bladder and prostate cancer (Khwaja et al., 2004). In addition, CD271 is hardly detected in invasive cutaneous squamous cell carcinoma (Dallaglio et al., 2014). In the last few years, contradictory results concerning CD271 as a marker of melanoma-initiating cells (MICs) have been published. It has been recently proposed that CD271 is an "imperfect marker" for MICs, because fast-growing CD271$^+$ cells exhibit poor tumorigenic ability (Cheli et al., 2014). To better understand the role of this receptor in melanoma, we studied CD271 in vitro by using three-dimensional (3D) multicellular spheroids and skin equivalents that closely mimic the behavior of solid tumors in vivo (Griffith and Swarz, 2006). We show the CD271$^-$ spheroids proliferate and invade more than CD271$^+$ spheroids. CD271 silencing induces both cell migration and proliferation, which are reduced when CD271 is overexpressed. Moreover, using a zebrafish melanoma model, we provide evidence that lack of CD271 is critical for melanoma progression, because it is associated with a higher number of metastases. Finally, we show a reduced expression of β_1-integrin and decreased cell-cell adhesion in the absence of CD271, resulting in poor tumor cell adhesion and in a greater predisposition to invade the microenvironment.

[1]*Laboratory of Cutaneous Biology, Department of Surgical, Medical, Dental and Morphological Sciences, University of Modena and Reggio Emilia, Modena, Italy;* [2]*Laboratory of Cell Biology and Advanced Cancer Therapies, Department of Medical and Surgical Sciences for Children & Adults, University of Modena and Reggio Emilia, Modena, Italy; and* [3]*Laboratory of Developmental Genetics, Department of Biology, University of Padova, Padova, Italy*

[4]*These authors contributed equally to the work.*

Correspondence: Carlo Pincelli, Laboratory of Cutaneous Biology, Department of Surgical, Medical, Dental and Morphological Sciences, University of Modena and Reggio Emilia, Via Del Pozzo 71, 41124 Modena, Italy. E-mail: carlo.pincelli@unimore.it

Abbreviations: 3D, three-dimensional; HIF-1α, hypoxia inducible factor-1α; MIC, melanoma-initiating cell; MM, metastatic melanoma; MTT, 3-(4,5-dimethylthiazol-2-yl)-2,5-diphenyltetrazolium bromide; PM, primary melanoma

Received 29 January 2016; revised 23 May 2016; accepted 31 May 2016; accepted manuscript published online 18 June 2016; corrected proof published online 27 July 2016

RESULTS

CD271 inversely correlates with melanoma progression stage and invasiveness in 3D spheroids

We recently showed that CD271 is markedly expressed in early-stage melanomas and that it is progressively lost during tumor progression, showing an inverse correlation with hypoxia inducible factor-1 (HIF-1α) (Marconi et al., 2015). Given this finding, we decided to study the role of CD271 in spheroids that mimic the 3D architecture and heterogeneity of melanoma (Beaumont et al., 2014). CD271 expression was evaluated in long-standing cell lines (WM115, WM266-4, SKMEL28, WM793-B, and 1205Lu) derived from melanomas of different stages and in cells freshly isolated from a primary melanoma (PM) and a metastatic melanoma (MM).

CD271 was significantly decreased in MM compared with the PM derived from the same patient (Figure 1a). The same behavior is observed in long-standing cell lines: primary WM115 and WM793-B cells express higher levels of CD271 than their metastatic counterparts (WM266-4 and 1205Lu, respectively). CD271 levels in the primary tumors were highly variable (WM115, SKMEL28, WM793-B, and PM), thus mirroring the great interpatient heterogeneity of this tumor. The same heterogeneity was observed in the metastases (WM266-4, 1205Lu, and MM). The levels of CD271

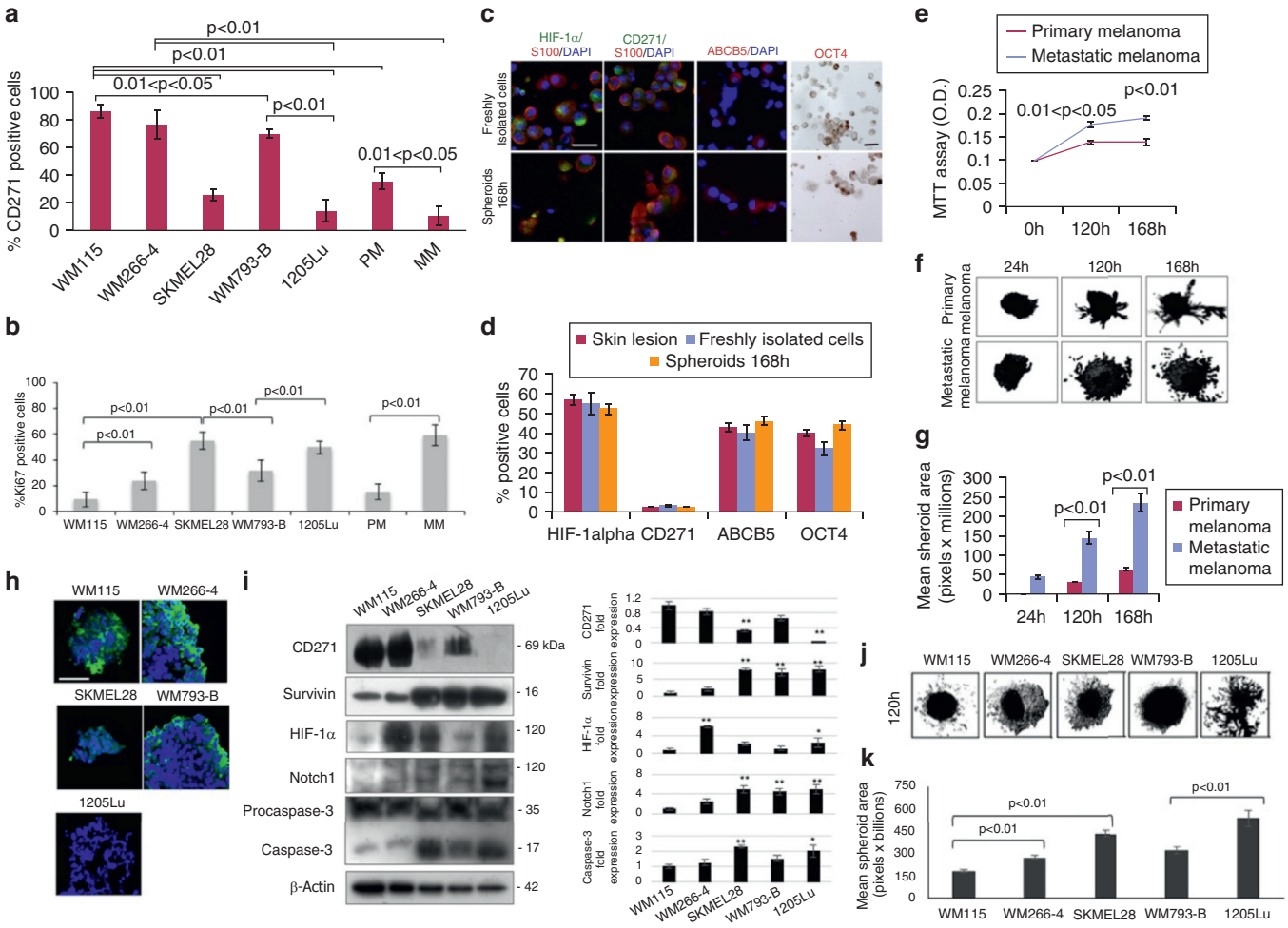

Figure 1. CD271 inversely correlates with melanoma progression stage and invasiveness in 3D spheroids. (**a**) Melanoma cells obtained from spheroids were immunostained with anti-CD271 MoAb and analyzed by flow cytometry. (**b**) Spheroids were harvested and cytospinned, and immunohistochemical detection of Ki67 was performed by using Fast Red as the chromogen. The number of positive cells was counted in six independent fields, and Ki67 level was calculated as the average percentage of positive cells. (**c**) Cells isolated from melanoma biopsy samples were used to obtain freshly isolated cells and spheroids were grown up to 168 hours. Cells were cytospinned, and immunohistochemistry of different markers was performed. Scale bar = 50 μm. (**d**) The percentage of positive cells in spheroids and in freshly isolated cells was compared with the same skin lesion. (**e**) Cells freshly isolated from a primary and a metastatic tumor were cultured as 3D spheroids, and MTT assay was performed at different times. (**f**) Pictures of spheroids implanted into type I collagen were analyzed and (**g**) total areas were calculated by using ImageJ software (see picture analysis in Supplementary Materials online). (**h**) Twenty spheroids for each cell line were stained with anti-CD271 MoAb for 3D confocal analysis. Scale bar = 100 μm. (**i**) Proteins extracted from melanoma spheroids 168 hours after seeding were immunoblotted with CD271, survivin, HIF-1α, Notch1, caspase-3, and β-actin antibody. The band intensity was quantitatively determined using ImageJ software (Wayne Rasband, see picture analysis in Supplementary Materials). Protein level intensity was normalized to β-actin expression. *$0.01 < P < 0.05$; $^{**}P < 0.01$. (**j**) Spheroids were implanted into a scaffold of type I collagen, and (**k**) pixel analysis was performed to calculate total area. Data represent the mean ± standard deviation of triplicate determinations, and Student *t* test was used for statistical analysis. 3D, three dimensional; h, hours; HIF-1α, hypoxia inducible factor-1α; MM, metastatic melanoma; MoAB, monoclonal antibody; MTT, 3-(4,5-dimethylthiazol-2-yl)-2,5-diphenyltetrazolium bromide; O.D., optical density; PM, primary melanoma.

were significantly higher in the WM266-4 cell line derived from a dermal metastasis than in 1205Lu and MM cells that originated from lung metastases.

Furthermore, the percentage of the melanoma predictor of proliferation Ki67 was higher in cells expressing the lowest levels of CD271 (SKMEL28, 1205Lu, and MM) (Figure 1b). To confirm the ability of spheroids to reflect the behavior of tumors in vivo, cells isolated from primary melanomas were seeded and characterized in vitro. Markers of melanoma (HIF-1α, CD271, ABCB5, and Oct4) were maintained in spheroids for up to 168 hours, and they were comparable to those observed in skin lesions and in cells freshly isolated from the same patient (Figure 1c and d). Finally, MM spheroids proliferated more than PM spheroids, as shown by 3-(4,5-dimethylthiazol-2-yl)-2,5-diphenyltetrazolium bromide (MTT) assay (Figure 1e), replicating the growth of the tumor in vivo. Spheroids were then implanted into a matrix of collagen I, which mimics the tumor microenvironment (Figure 1f). Areas occupied by the cells showed greater invasion abilities in MM than in PM spheroids (Figure 1g). Confocal microscopy confirmed that CD271 (green) was barely detectable in SKMEL28 and 1205Lu spheroids (Figure 1h), also shown by Western blotting (Figure 1i). Indeed, survivin and Notch1, involved in melanoma progression, were more expressed in SKMEL28, WM793-B, and 1205Lu cells than in less-aggressive cell lines. In addition, the amount of active caspase-3, which promotes migration and invasion of nonapoptotic melanoma cells (Liu et al., 2013), was higher in SKMEL28 and 1205Lu than in the other spheroids. HIF-1α level was higher in spheroids derived from advanced-stage melanomas (WM266-4 and 1205Lu) (Figure 1i). In addition, metastatic WM266-4 and 1205Lu spheroids invaded more than their primary counterparts (WM115 and WM793-B, respectively) (Figure 1j and k), and spheroids expressing the lowest levels of CD271 (SKMEL28 and 1205Lu) displayed the greatest invasive phenotype (Figure 1k). These data indicate that CD271 inversely correlates with melanoma progression and in vitro invasiveness.

CD271 is associated with poor invasiveness in spheroids and skin equivalents

To evaluate the role of CD271 in melanoma invasiveness, spheroids were transferred into collagen I, and CD271 expression was evaluated by immunohistochemistry. In all cell lines, most CD271$^+$ cells were noninvasive (Figure 2a). Consistently, cells expressing CD271 remained mostly confined to the body of the sphere (Figure 2b). Most invading cells were CD271$^-$, indicating a greater predisposition to invade the microenvironment (Figure 2c). To confirm these data in a model that better reflects the in vivo tissue architecture, cells were used to generate 3D skin equivalents. Melanoma reconstructs recapitulated tumor pathology, as shown by hematoxylin and eosin and S100 staining (Figure 2d). WM115 and WM266-4 cells were confined to the epidermis, whereas SKMEL28, WM793-B, and 1205Lu

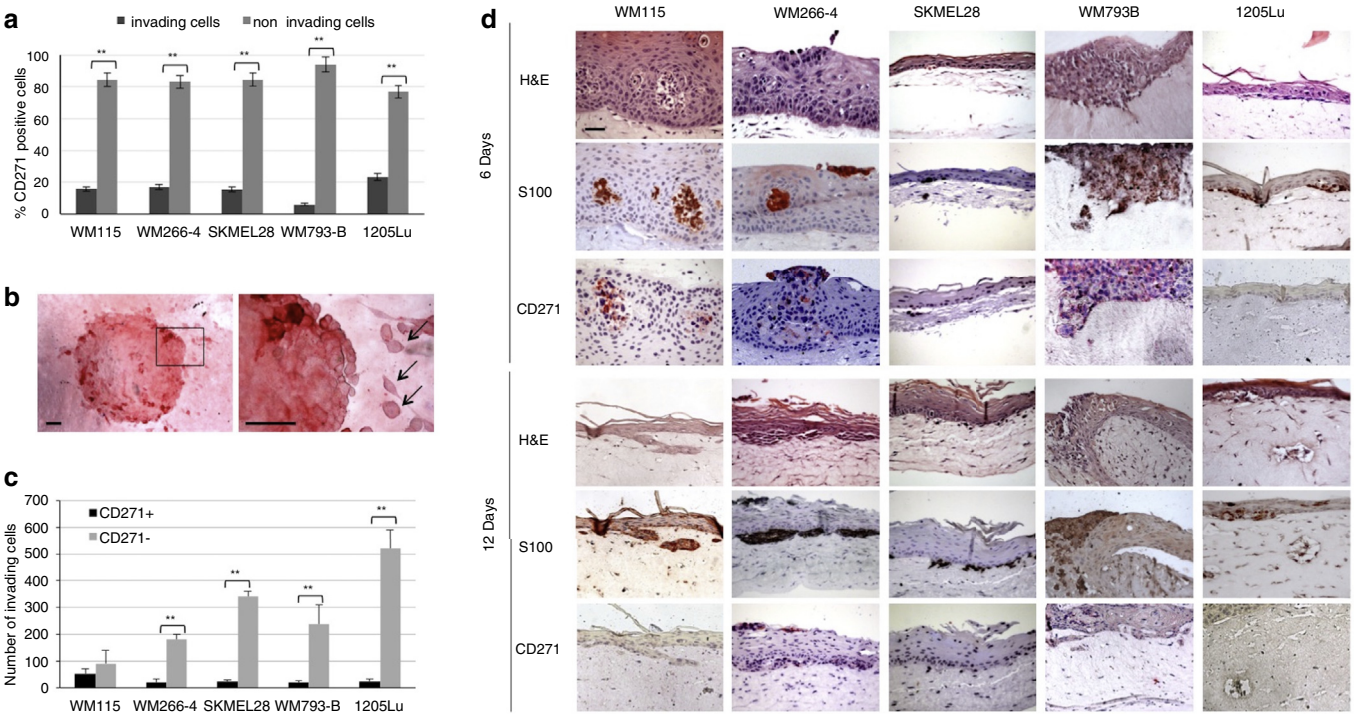

Figure 2. CD271 is associated with poor invasiveness in spheroids and skin equivalents. (**a**) Melanoma spheroids were implanted into type I collagen and stained 72 hours later with CD271 MoAb. Fast Red was used as the chromogen. Cells were counted using ImageJ software (see picture analysis in Supplementary Materials). (**b**) Pictures were used to count CD271$^+$ cells (red) and CD271$^-$ cells (arrows). Scale bars = 30 μm (right) and 120 μm (left, zoom). (**c**) Invading cells are all the cells outside the spheroid and embedded in collagen I. Noninvading cells are those located within the body of the sphere. Among invasive cells, CD271$^+$ and CD271$^-$ cells were counted. Data represent the mean ± standard deviation of triplicate determinations, and Student *t* test was used for statistical analysis. *$0.01 < P < 0.05$; **$P < 0.01$ (**d**) Skin reconstructs, obtained as described in the Materials and Methods, were paraffin-embedded after either 6 or 12 days of submersion. Sections were stained with hematoxylin and eosin, CD271, and S100 MoAb. Fast Red for CD271 or DAB for S100 were used as chromogens. Scale bar = 100 μm. DAB, 3,3′-diaminobenzidine; MoAb, monoclonal antibody.

cells localized at the dermal-epidermal junction at 6 days after plating. All melanoma cells invaded the dermis at 12 days after seeding. At day 6, CD271 expression was detected only in WM115−, WM266-4−, and WM793-B−derived reconstructs, and it decreased or disappeared during progression to 12 days in skin equivalents originating from the same cell lines. By contrast, CD271 was not expressed in reconstructs derived from SKMEL28 and 1205Lu cells either at 6 or 12 days (Figure 2d). Taken together, these data confirm an inverse correlation between the CD271 receptor and melanoma invasiveness.

CD271$^-$ spheroids display increased proliferation and invasion abilities

To better understand the role of CD271 in melanoma, we isolated SKMEL28 CD271$^+$ and CD271$^-$ cells (see Supplementary Figure S1a and b online) that were seeded as spheroids (see Supplementary Figure S2a online). CD271$^+$ spheroids proliferated significantly less than CD271$^-$ spheroids from 72−168 hours (Figure 3a). Analysis of pictures (Figure 3b) showed that the area of CD271$^-$ spheroids increased in a time-dependent manner, whereas it remained unchanged in CD271$^+$ spheroids (Figure 3c). Given that CD271 is used as a marker of cancer stem cells, the possibility that CD271$^-$ cells exhaust earlier than CD271$^+$ cells was also evaluated: spheroids were grown for 7 days, dissociated, counted, and replated under the same conditions in a long-term assay. Despite both CD271$^-$ and CD271$^+$ spheroids propagating during serial passages, the number of cells derived from CD271$^-$ spheroids was always higher than from CD271$^+$ spheroids (Figure 3d). On the other hand, 30% of CD271$^+$ spheroids expressed the pluripotency marker Oct4, whereas its expression was absent in CD271$^-$ spheroids (Figure 3e). WM793-B cells were also sorted (see Supplementary Figure S1c and d) and cultured as 3D spheroids (see Supplementary Figure S2c). The calculation of areas (see Supplementary Figure S2d and e), MTT (see Supplementary Figure S2f), long-term growth (see Supplementary Figure S2g), and Oct4 levels (see Supplementary Figure S2h) yielded the same findings.

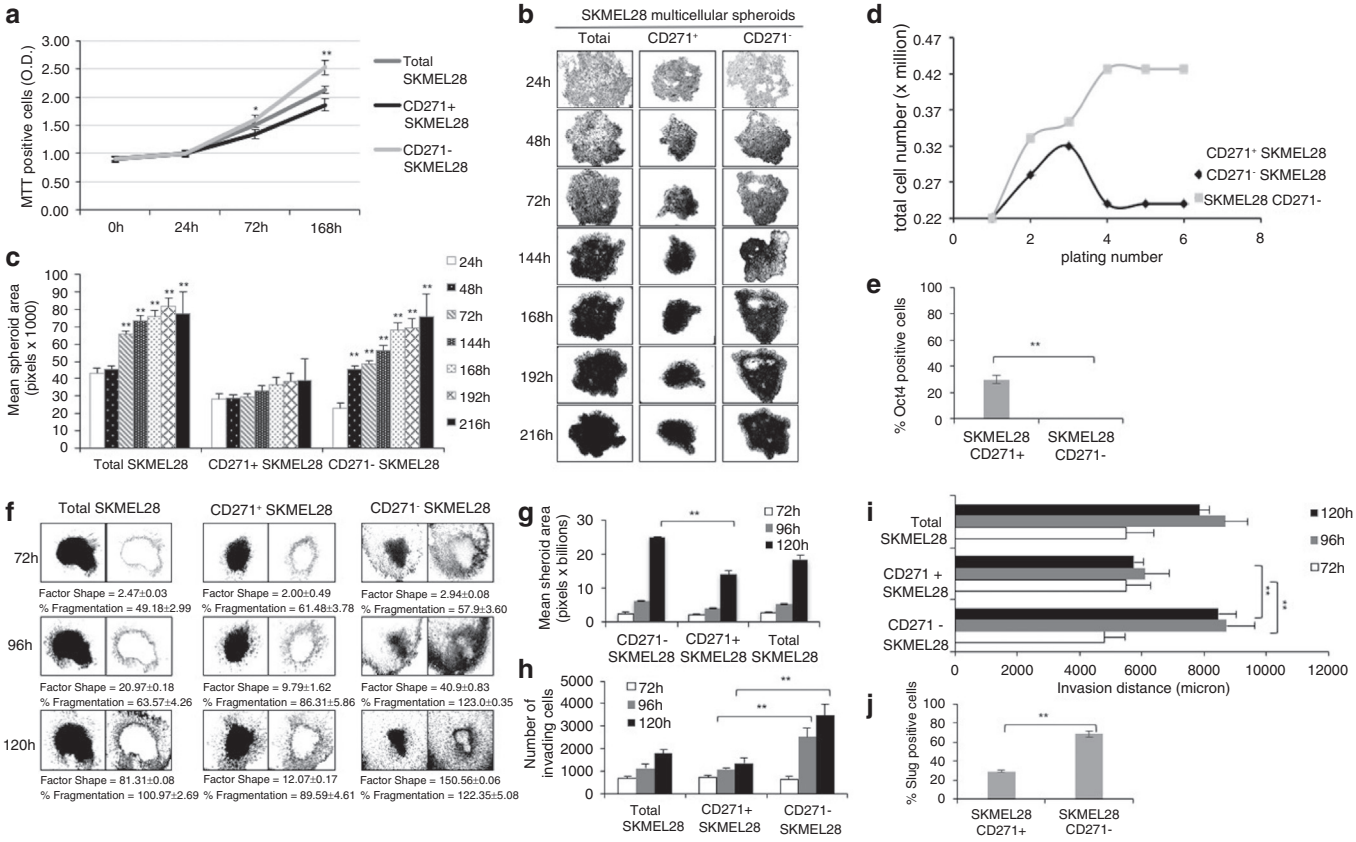

Figure 3. CD271$^-$ spheroids display increased proliferation and invasion abilities. (**a**) CD271$^+$ and CD271$^-$ SKMEL28 subpopulations were cultured up to 168 hours after seeding, and MTT assay was performed at different times. (**b**) Pictures of spheroids were converted to 8-bit, and (**c**) were analyzed with ImageJ software for the calculation of total area (see picture analysis in Supplementary Materials). (**d**) CD271$^+$ and CD271$^-$ cells were grown for 7 days as spheroids, dissociated, counted, and replated under the same conditions in a long-term assay. (**e**) CD271$^+$ and CD271$^-$ cells were fixed and cytospinned immediately after cell sorting. Immunohistochemical detection of Oct4 was performed by using Fast Red as the chromogen. The number of positive cells was counted in six independent fields, and Oct4 level was calculated as the average percentage of positive cells. (**f**) Pictures of CD271$^+$ and CD271$^-$ SKMEL28 spheroids implanted into type I collagen were analyzed up to 120 hours, and factor shape, percentage of fragmentation and (**g**) total areas were calculated with ImageJ software (see picture analysis in Supplementary Materials). (**h**) Total number of invading cells was counted with the ImageJ Cell Counter (see picture analysis in Supplementary Materials). (**i**) Distances reached by the cells in type I collagen was evaluated by using Photoshop, considering cells migrated in the directions of the four cardinal points. The average distance was calculated and the number of pixels were converted into micron (see Materials and Methods). (**j**) Immunohistochemical detection of Slug was performed after cell sorting. The percentage of positive cells was calculated by counting six independent fields. Data represent the mean of triplicate determinations. Student *t* test was used for statistical analysis. *$0.01 < P < 0.05$; **$P < 0.01$. h, hours; MTT, 3-(4,5-dimethylthiazol-2-yl)-2,5-diphenyltetrazolium bromide; O.D., optical density.

SKMEL28 spheroids were then implanted into type I collagen and monitored (see Supplementary Figure S2b). CD271$^-$ spheroids invaded significantly more frequently than CD271$^+$ spheroids. Factor shape and percentage of fragmentation, two values correlated with melanoma invasiveness, were higher in CD271$^-$ than CD271$^+$ spheroids (Figure 3f). In addition, CD271$^-$ spheroids occupied a greater area (Figure 3g) and displayed a higher number of invading cells (Figure 3h) than their positive counterpart. Calculation of the distance showed that CD271$^-$ spheroids achieved greater distances than CD271$^+$ cells in collagen at 96 and 120 hours (Figure 3i). Consistently, the epithelial-mesenchymal transition factor Slug, which promotes melanoma invasion (Fenouille et al., 2012), was more expressed in CD271$^-$ cells. Results are confirmed in WM793-B cells (see Supplementary Figure S2i, j, k, and l).

CD271 silencing enhances proliferation and invasiveness in melanoma spheroids

To evaluate whether the absence of CD271 was responsible for a more aggressive phenotype in vitro, we silenced CD271 in WM115 cells, which express a high level of the receptor (Figure 4a). Transfected cells were seeded to obtain spheroids (see Supplementary Figure S3a online). First, after CD271 silencing, survivin increased, as a function of increased aggressiveness (Figure 4a). Image analysis (Figure 4b) showed higher areas in CD271-silenced spheroids at up to 120 hours compared with scramble cells (Figure 4c), indicating an

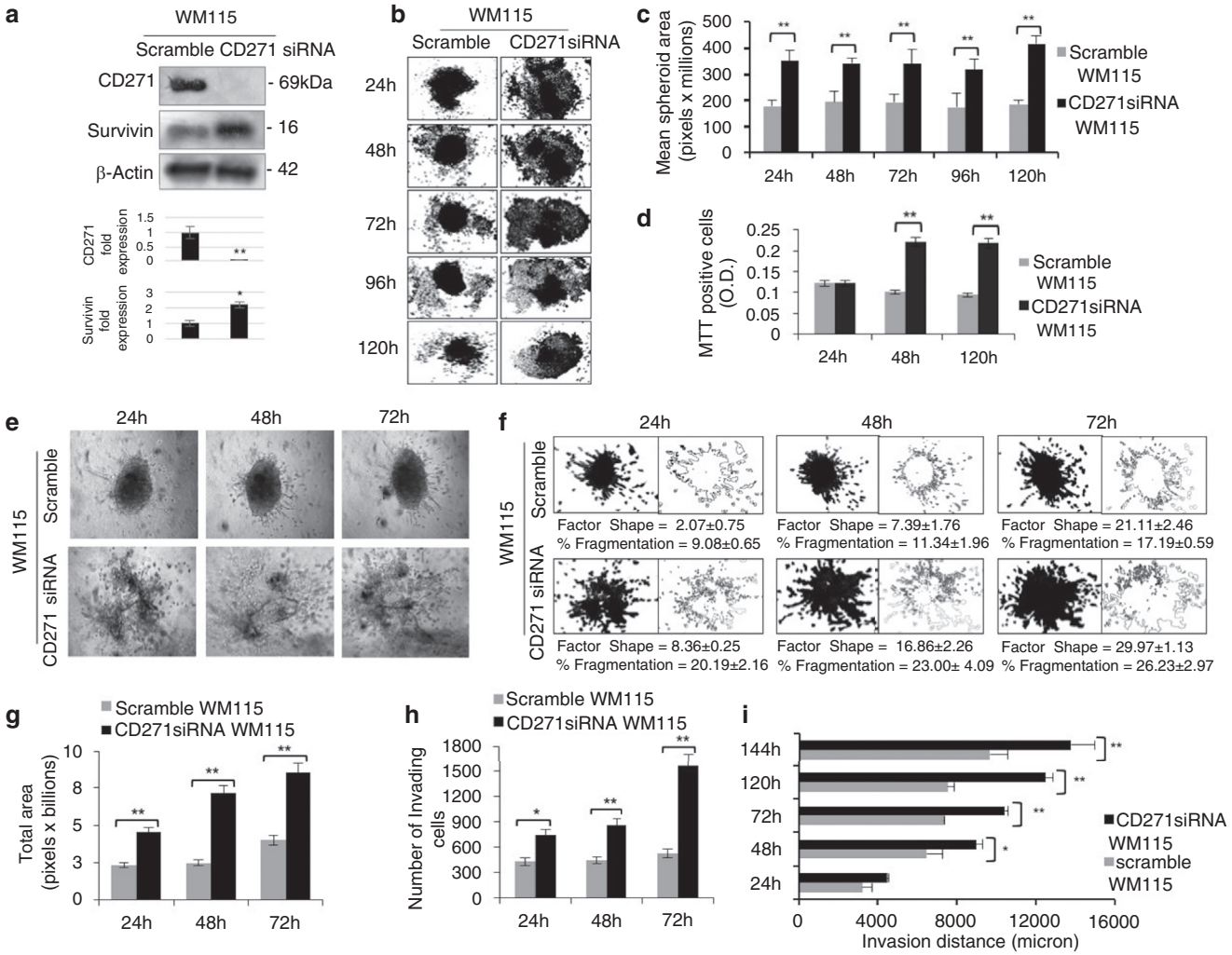

Figure 4. CD271 silencing enhances proliferation and invasiveness in melanoma spheroids. (**a**) WM115 cells were transfected with 50 nmol/L CD271 siRNA, and protein extracts were immunoblotted with CD271 and survivin MoAb. The band intensity was quantitatively determined using ImageJ software (Wayne Rasband, see graphs below the immunoblot and Supplementary Materials). Protein level intensity was normalized to β-actin expression. *$0.01 < P < 0.05$; **$P < 0.01$. (**b**) Pictures of spheroids were converted in 8-bit, and (**c**) pixel analysis was performed with ImageJ to calculate total area (see picture analysis in Supplementary Materials). (**d**) MTT assay at different times. (**e**) WM115 cells were transfected with scramble and CD271 siRNA and seeded as spheroids; 72 hours later, spheroids were implanted into type I collagen, and pictures were taken at different times. (**f**) Factor shape and the percentage of fragmentation were calculated (see Materials and Methods). (**g**) Pixel analysis was performed to calculate total area (see Materials and Methods). (**h**) Invading cells were counted with ImageJ (see picture analysis in Supplementary Materials). (**i**) Distances reached by cells in type I collagen were evaluated (see Materials and Methods). Data represent the mean ± standard deviation of triplicate determinations. Student *t* test was used for statistical analysis. *$0.01 < P < 0.05$; **$P < 0.01$. h, hours; MoAb, monoclonal antibody; MTT, 3-(4,5-dimethylthiazol-2-yl)-2,5-diphenyltetrazolium bromide; O.D., optical density; siRNA, small interfering RNA.

increased proliferation, which was confirmed by MTT (Figure 4d). CD271 silencing yielded the same results in WM793-B cells (see Supplementary Figure S3b, c, d, and f).

Twenty-four hours after implantation into collagen I, CD271 silencing induced a marked change in spheroids, which appeared disgregated into single cells, not scrambled cells (Figure 4e). This reflects a greater invasiveness, as shown by the increase in factor shape, percentage of fragmentation (Figure 4f), and total area (Figure 4g). Moreover, CD271 silencing resulted in a higher number of cells invading type I collagen (Figure 4h) and reaching higher distances than controls (Figure 4i). Taken together, these data suggest that lack of CD271 is associated with greater proliferation and invasion ability.

CD271 overexpression decreases tumor proliferation and invasiveness in melanoma spheroids

Because the absence of CD271 correlates with greater invasion and proliferation, we asked whether its overexpression could revert melanoma to a less aggressive phenotype. To test this, SKMEL28 cells were infected with a CD271 or mock viral vector, and spheroids were monitored (see Supplementary Figure S4a online). First, CD271 overexpression caused a down-regulation of the markers of invasion Slug and caspase-3 (Figure 5a). Pictures (Figure 5b) showed a slight decrease in the total areas occupied by CD271-infected spheroids (Figure 5c). Moreover, CD271-overexpressing spheroids proliferated significantly less than mock cells (Figure 5d). Given that CD271 receptor mediates apoptosis in many cell settings, we evaluated whether the reduced viability was associated with the activation of the apoptotic cascade. However, the percentage of apoptotic cells failed to increase in CD271-overexpressing cells (Figure 5e and f). CD271-overexpressing spheroids were then implanted into collagen I (see Supplementary Figure S4b), displaying a reduced invasiveness, as shown by the decrease in factor shape and percentage of fragmentation (Figure 5g). Consistently, the total area (Figure 5h) and the area of invasion were significantly reduced in CD271-overexpressing spheroids compared with controls (Figure 5i). Finally, they reached a lower distance in collagen I than mock spheroids (Figure 5j). The same results were obtained by infecting the 1205Lu cell line (see Supplementary Figure S4c–i).

The lack of CD271 favors tumor metastasis in zebrafish and is associated with a reduced cell-cell adhesion

The zebrafish model has recently contributed to major insights in the progression of melanoma (Kaufman et al., 2016; White et al., 2013). To definitely confirm the role of CD271 in melanoma, we evaluated the ability of zebrafish to mirror the metastatic process. Primary WM115 and metastatic 1205Lu cells (red) were injected into transparent larvae, and the spread of cells was evaluated 6 days later (see Supplementary Figure S5a and b online). Larvae were xenotransplanted under three different conditions: (i) CD271$^+$ and CD271$^-$ cells sorted from SKMEL28 cell lines (Figure 6a–d), (ii) WM115 cells silenced for CD271 (Figure 6e–g), and (iii) CD271–overexpressing 1205Lu cells (Figure 6h–j). At day 2, cells were confined to the site of injection (yolk), and at 6–7 days postinjection the number of metastases was markedly increased in SKMEL CD271$^-$ cells (Figure 6a and b) and in WM115 CD271-silenced cells (Figure 6e and f) compared

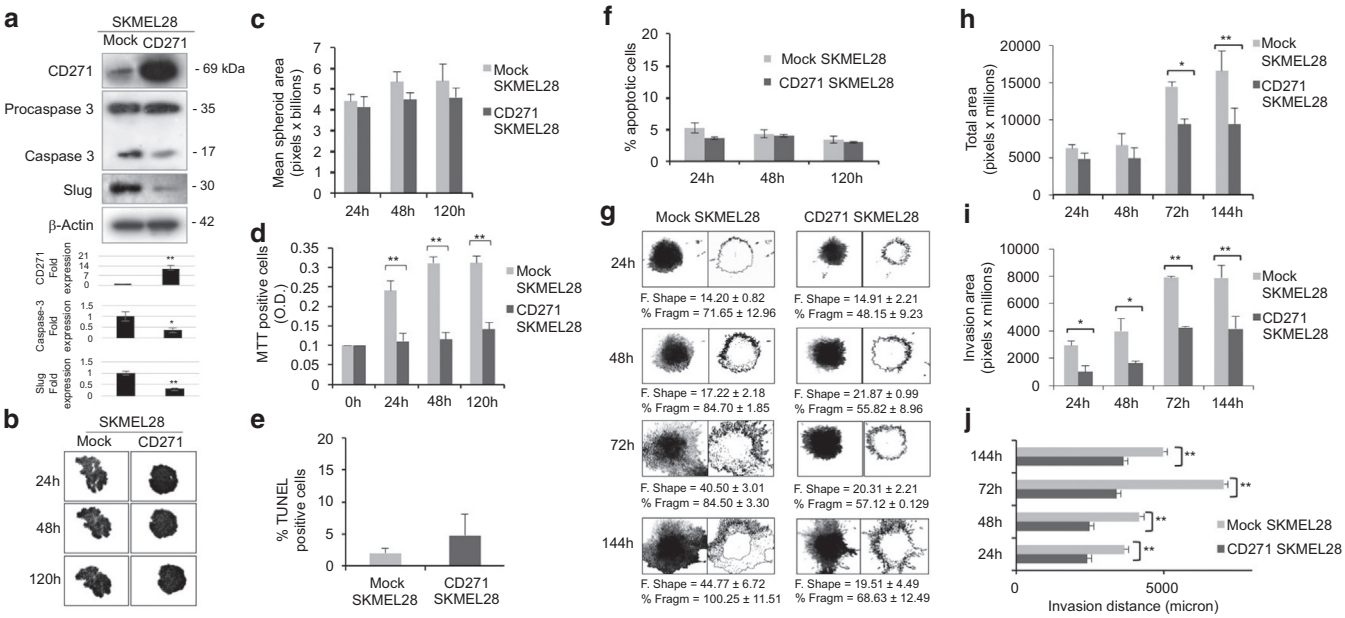

Figure 5. CD271 overexpression decreases tumor proliferation and invasiveness in melanoma spheroids. (**a**) SKMEL28 cells were infected with mock or CD271 retroviral vector, and cell lysates were immunoblotted. The band intensity was quantitatively determined using ImageJ software (Wayne Rasband, see picture analysis in Supplementary Materials). Protein level intensity was normalized to β-actin expression. *$0.01 < P < 0.05$; **$P < 0.01$. (**b**) SKMEL28 spheroids pictures were converted with ImageJ. (**c**) Pixel analysis was performed to calculate total areas (see Materials and Methods). (**d**) MTT assay. (**e, f**) Apoptotic cells of SKMEL28 mock and CD271 infected spheroids were evaluated by TUNEL and PI assay. (**g**) CD271 infected and mock treated spheroids were implanted into a scaffold of type I collagen. Factor shape, percentage of fragmentation, (**h**) total area and (**i**) invasion area were calculated (see Materials and Methods). (**j**) Distances reached by SKMEL28 cells into type I collagen. The average distance was calculated (see Materials and Methods). Data represent the mean ± standard deviation of triplicate determinations. Student *t* test was used for statistical analysis. *$0.01 < P < 0.05$; **$P < 0.01$. h, hours; MTT, 3-(4,5-dimethylthiazol-2-yl)-2,5-diphenyltetrazolium bromide; PI, propidium iodide.

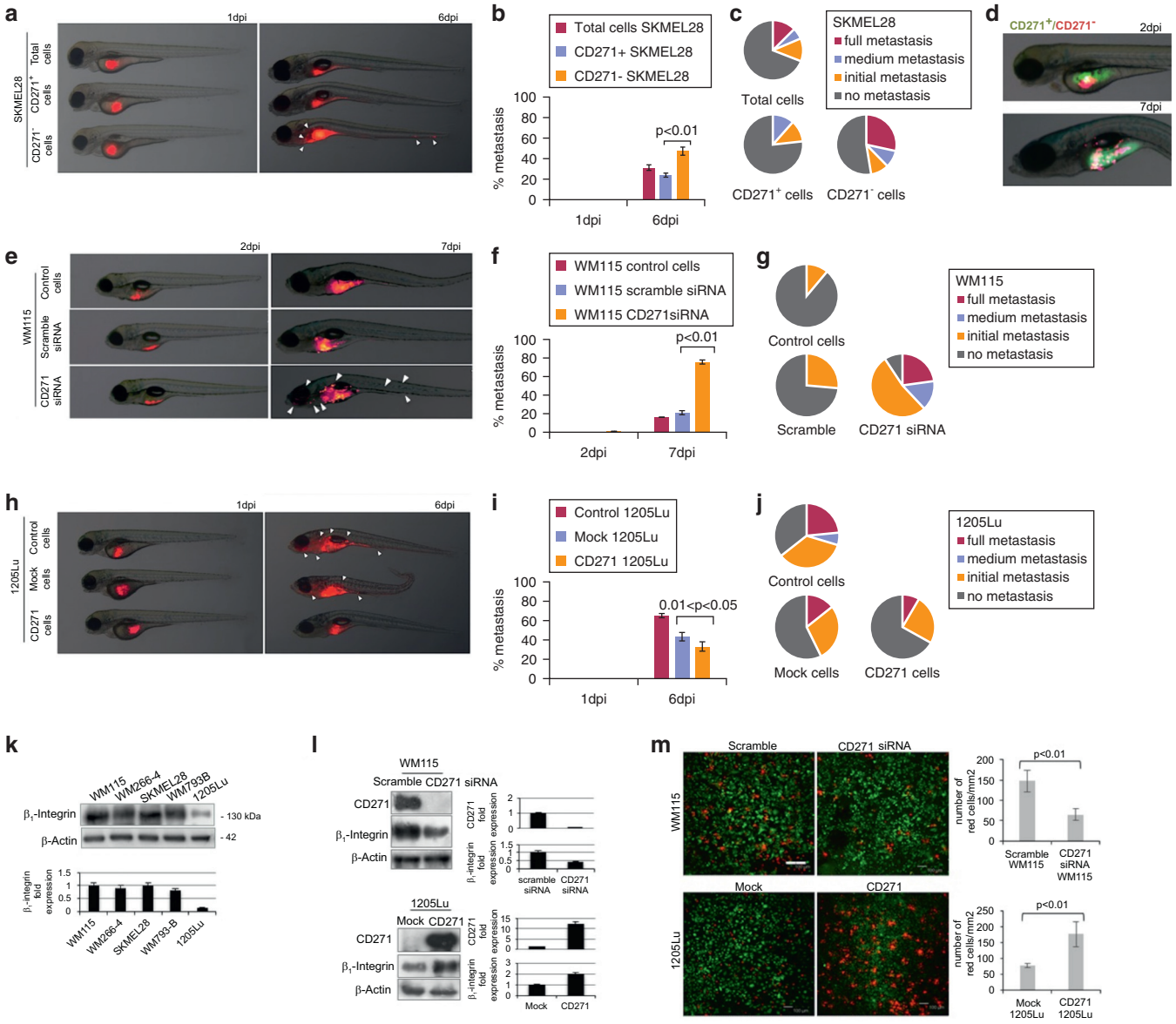

Figure 6. The lack of CD271 favors tumor metastasis in zebrafish and is associated with a reduced cell-cell adhesion. (**a**) CD271$^+$ and CD271$^-$ SKMEL28 subpopulations were stained with Vybrant Cell Labeling Solution (ThermoFisher, Waltham, MA) (red), injected into the yolk of transparent zebrafish larvae at 2 dpf and monitored. (**b**) The number of embryos with metastases was counted at 1 dpi and 6 dpi. (**c**) The percentage of zebrafish with full metastasis (>10 cells), medium metastasis (5−10 cells), and initial metastasis (2−4 cells) was calculated. (**d**) SKMEL28 CD271$^+$ (green, stained with CFSE) and CD271$^-$ (red, stained with Vybrant Cell Labeling Solution) cells were injected together in zebrafish larvae, and pictures were taken at 2 dpi and 7 dpi. (**e**) WM115 scramble and CD271 siRNA cells (red) were injected into zebrafish at 2 dpf, and (**f**) the number and (**g**) the severity of metastases were calculated at 2 dpi and 7 dpi. (**h**) 1205Lu mock and CD271 infected cells (red) were injected into transparent larvae. (**i**) The percentage of metastasis was calculated at 1 dpi and 6 dpi. (**j**) Full, medium, and initial metastases were evaluated. (**k, l**) Proteins extracted from melanoma spheroids 168 hours after seeding were immunoblotted with β_1-integrin and β-actin. The band intensity was quantitatively determined using ImageJ software (Wayne Rasband, see picture analysis in Supplementary Materials). Protein level intensity was normalized to β-actin expression. *$0.01 < P < 0.05$; **$P < 0.01$. (**m**) For the cell-cell adhesion assay, the same cells were stained with Vybrant Cell Labeling Solution (red) and CFSE (green). WM115 scramble and CD271 siRNA cells stained with CFSE (green) were grown as monolayer. WM115 scramble and CD271 siRNA cells stained with Vybrant Cell Labeling Solution (red) were plated on the corresponding monolayer and incubated for 40 minutes at 37 °C. After washing the unbound cells, the number of red cells/mm^2 were counted (see Materials and Methods). The same experiment was performed for 1205Lu mock and CD271-infected cells. Scale bar = 20 μm. CFSE, carboxyfluorescein succinimidyl ester; dpi, days postinjection; dpf, days postfertilization; siRNA, small interfering RNA.

with CD271$^+$ and control cells, respectively. The same result was observed when SKMEL28 CD271$^+$ (green) and CD271$^-$ (red) cells were injected together (Figure 6d). On the contrary, the percentage of metastases decreased at 6 days post-injection of CD271-overexpressing 1205Lu cells (Figure 6h and i). A higher number of "full" (>10 cells) and "medium" (5−10 cells) metastases were observed in the absence of CD271, whereas zebrafish injected with SKMEL28 CD271$^+$ (Figure 6c), WM115 scramble (Figure 6g), and CD271-infected 1205Lu cells (Figure 6j) displayed mostly "initial metastasis" (2−4 cells).

Finally, to better understand the mechanism underlying the role of CD271 in melanoma progression, we hypothesized that there is a correlation between adhesion molecules and CD271 levels. The observation that CD271 silencing in WM115 spheroids (Figure 4) was associated with a less

compact shape suggests that the lack of CD271 could be related to a decrease in cell-cell adhesion, thus increasing the predisposition to invade. We show that β_1-integrin was reduced in the metastatic WM266-4 and 1205Lu cells (Figure 6k). In addition, CD271 silencing caused β_1-integrin down-regulation, and CD271 overexpression correlated with increased levels of the protein (Figure 6l). Finally, CD271-silenced WM115 cells displayed a reduced intercellular adhesion, as shown by the reduced number of adherent cells (red), whereas increased adhesion was observed in CD271-overexpressing 1205Lu cells (Figure 6m). These results show that the lack of CD271 favors tumor metastasis in vivo and that CD271 is correlated with cell-cell adhesion.

DISCUSSION

The present study provides data that shed light on the function of CD271 in melanoma progression. Using 3D spheroids, we showed that CD271 is inversely correlated to the invasiveness and growth of the tumor. CD271 decreased during progression from primary to metastatic melanoma in the same patient. When spheroids were implanted into a matrix of collagen I, CD271 was highly expressed in cells confined to the body of the sphere, but it was almost absent in cells that detached from the sphere to invade. These results seem to be in contrast with previous publications that reported a role of neurotrophins in mediating melanoma cell invasion and migration (Marchetti et al., 1998; Truzzi et al., 2008). Because early studies were carried out in two-dimensional cultures, we hypothesized that the conflicting results are attributable to the different systems. Multicellular spheroids mimic the 3D architecture and heterogeneity of melanoma by recreating the oxygen/nutrients gradient (Beaumont et al., 2014). Moreover, the genomic profile of glioma is preserved in spheroids but not in primary monolayer cultures (De Witt et al., 2009), whereas 3D models markedly affect gene expression in melanoma (Ghosh et al., 2005). Skin reconstructs are a good tool for studying tumor-microenvironment interactions (Vörsmann et al., 2013). Here, we show that CD271 is expressed in melanoma cells located in the epidermis of skin reconstructs but that it disappears when melanoma invades the dermis. Consistently, HIF-1α is present at great levels in tumors invading the dermis; CD271 is markedly expressed in early-stage melanomas, but it is progressively lost during progression (Marconi et al., 2015).

Contradictory results concerning CD271 and its use as a marker to isolate MICs have been recently published. Boiko (2010) showed that MICs can be isolated as a highly enriched CD271 population. Moreover, CD271/Sox10-positive melanoma cells have been associated with higher metastatic potential (Civenni et al., 2011). On the contrary, melanoma can metastasize in mice irrespective of whether they derive from CD271$^+$ or CD271$^-$ cells (Quintana et al., 2010). In this article, we show that CD271$^+$ cells are slow-growing cells that display increased levels of the stemness marker Oct4. On the other hand, both CD271$^+$ and CD271$^-$ spheroids display a long-term growth. Moreover, CD271 is regulated by hypoxic and stringent culture conditions (Menon et al., 2015), and its detectability is affected by the tumor digestion protocol. Most studies were carried out in spheroids maintained in a stem cell medium that select a subpopulation with stemness properties (Ramgolam et al., 2011). Here, spheroids were obtained according to the liquid overlay method that preserves tumor heterogeneity. Finally, biopsy samples were processed with a protocol that avoids the damage of surface epitopes. In substance, although we do not aim to fully address the correlation between CD271 and MICs in this article, the high percentage of CD271$^+$ cells in primary melanomas seems to rule out their stem nature. Whether a subpopulation of CD271$^+$ cells could contain MICs remains to be determined.

The inverse correlation between CD271 expression and melanoma progression was further confirmed by using a zebrafish model. The zebrafish has recently emerged as an important model in cancer research able to develop human tumors, with similar morphology and comparable signaling pathways (Heilmann et al., 2015; Kaufman et al., 2016). Here, we show that the lack of CD271 is critical for melanoma progression in vivo. When injected into zebrafish, CD271-silenced WM115 cells, SKMEL28 CD271$^-$ cells, and 1205Lu mock cells provoked a higher number of metastases compared with cells expressing higher amounts of CD271. Consistently, spheroids acquired a more invasive phenotype in the absence of CD271, as also shown by the increase of Slug and caspase 3 levels. Because SKMEL28 spheroids failed to undergo apoptosis after CD271 overexpression, the activation of caspase-3 is consistent with its ability to promote invasion (Donato et al., 2014; Liu et al., 2013).

CD271 silencing down-regulated β_1-integrin and reduced cell-cell adhesion, and its overexpression in 1205Lu induced β_1-integrin up-regulation and an increase in cell-cell adhesion. It is known that $\alpha_4\beta_1$-integrin inhibits metastases, and it is involved in intercellular adhesion (Qian et al., 1994). Moreover, Slug is associated with loss of cell-cell adhesion mediated by E-cadherin in melanoma (Shirley et al., 2012). This suggests that CD271 down-regulation promotes melanoma progression and invasion at least in part because of the lack of cell-cell adhesion. However, further experiments are required to identify the molecules that take part in this process. In conclusion, we hypothesize that a melanoma subpopulation needs to turn off CD271 to acquire the ability to invade during the early stages of melanoma progression.

MATERIALS AND METHODS

Cell culture

WM115, WM266-4, SKMEL28, WM793B, and 1205Lu (ATCC, Manassas, VA) were cultured as indicated by the manufacturer. MTT, liquid overlay method, invasion assay, picture analysis, and long term growth were performed as indicated in the Supplementary Materials online. Melanoma biopsy samples were processed as described in the Supplementary Materials.

FACS

Spheroids incubated with anti-CD271 antibody (1:100 in phosphate buffered saline, Lab Vision Corporation, ThermoFisher Scientific, Fremont, CA) for 20 minutes at 4 °C were labeled with secondary antibody Alexa Fluor anti-mouse 488 (1:50, ThermoFisher Scientific) for 20 minutes at 4 °C. Cells were analyzed with Coulter Epics XL Flow Cytometer (Beckman Coulter, Brea, CA).

Skin reconstructs

Reconstructs were obtained by seeding human keratinocytes and melanoma cells on dermal equivalents generated by fibroblast-induced type I collagen contraction, as described in the Supplementary Materials.

Western blotting

Spheroids were harvested 48 or 72 hours after seeding, and Western blotting was performed as previously described (Tiberio et al., 2002) and indicated in the Supplementary Materials.

Immunohistochemistry

Skin reconstructs and skin lesions were stained with hematoxylin and eosin, S100 (1:400; Dako, Agilent Technologies, Dako Denmark A/S, Glostrup, Denmark), CD271 (1:100 in phosphate buffered saline, Lab Vision Corporation), ABCB5 (1:100 in phosphate buffered saline, ThermoFisher Scientific), Hif-1α (1:50 in phosphate buffered saline, Novus, Cambridge, UK), and Oct4 (1:100, Abcam, Cambridge, UK) as described in the Supplementary Materials. Spheroids in collagen I were fixed in 4% formalin for 30 minutes before CD271 detection. Sorted cells were fixed and stained with Slug (1:100, Histo-Line Laboratories, Milano, Italy) and Oct4 (1:100, Abcam) as indicated in the Supplementary Materials.

Cell sorting

Cells were sorted for CD271 expression by FACS sorter as described in the Supplementary Materials.

Cells transfection

Cells plated for 24 hours in antibiotic-free medium were transfected with CD271 or scrambled small interfering RNA (Dharmacon, Lafayette, CO) in antibiotic/fetal bovine serum-free medium, supplemented with 0.1% BSA as previously described (Truzzi et al., 2011) and indicated in the Supplementary Materials.

Cell infection

Spheroids were transduced by infection with viral supernatant generated by CD271-LNSN packaging cells or by empty vector packaging cells (kindly provided by F. Mavilio) as described in the Supplementary Materials.

Apoptosis evaluation

For TUNEL assay, spheroids were fixed in 4% paraformaldehyde and cytospinned. Slides were stained with the In Situ Cell Death Detection Kit (Roche Diagnostics, Basel, Switzerland) and analyzed by confocal laser microscopy as described in the Supplementary Materials. Spheroids were trypsinized and stained with propidium iodide (Milano, Italy) at different time points, as indicated in the Supplementary Materials.

Zebrafish

Larvae were injected at 2 days after fertilization with melanoma cells as indicated in the Supplementary Materials.

Cell-cell adhesion assay

Cell adhesion assay was performed as previously described (Qian et al., 1994) and indicated in the Supplementary Materials.

Statistical analysis

The Student *t* test was used, as indicated in the Supplementary Materials.

CONFLICT OF INTEREST

The authors state no conflict of interest.

ACKNOWLEDGMENTS

This work was partially supported by Fondazione Cassa di Risparmio di Modena, Italy. We thank Massimo Dominici for advice in cell sorting. NT is supported by AFM-Telethon (Project 18572 Polygon) and EU ZF-HEALTH, Italian Ministry of Health (RF-2010-2309484).

SUPPLEMENTARY MATERIAL

Supplementary material is linked to the online version of the paper at www.jidonline.org, and at http://dx.doi.org/10.1016/j.jid.2016.05.116.

REFERENCES

Beaumont KA, Kumaran NM, Haass NK. Modeling melanoma in vitro and in vivo. Healthcare 2014;2:27–46.

Blöchl A, Blöch R. A cell-biological model of p75NTR signaling. J Neurochem 2007;102:289–305.

Boiko AD, Razorenova OV, van de Rijn M, Swetter SM, Johnson DL, Ly DP, et al. Human melanoma-initiating cells express neural crest nerve growth factor receptor CD271. Nature 2010;466:133–7.

Cheli Y, Bonnazi VF, Jacquel A, Allegra M, De Donatis GM, Bahadoran P, et al. CD271 is an imperfect marker for melanoma initiating cells. Oncotarget 2014;5:5272–83.

Civenni G, Walter A, Kobert N, Mihic-Probst D, Zipser M, Belloni B, et al. Human CD271-positive melanoma stem cells associated with metastasis establish tumor heterogeneity and long-term growth. Cancer Res 2011;71:3098–109.

Dallaglio K, Petrachi T, Marconi A, Truzzi F, Lotti R, Saltari A, et al. Expression of nuclear survivin in normal skin and squamous cell carcinoma: a possible role in tumour invasion. Br J Cancer 2014;110:199–207.

De Witt Hamer PC1, Leenstra S, Van Noorden CJ, Zwinderman AH. Organotypic glioma spheroids for screening of experimental therapies: how many spheroids and sections are required? Cytometry A 2009;75:528–34.

Donato AL, Huang Q, Liu X, Li F, Zimmerman MA, Li CY. Caspase 3 promotes surviving melanoma tumor cell growth after cytotoxic therapy. J Invest Dermatol 2014;134:1686–92.

Eggermont AM, Spatz A, Robert C. Cutaneous melanoma. Lancet 2014;383:816–27.

Fenouille N, Tichet M, Dufies M, Pottier A, Mogha A, Soo JK, et al. The epithelial-Mesenchymal Transition (EMT) regulatory factor SLUG (SNAI2) is a downstream target of SPARC and AKT in promoting melanoma cell invasion. PLoS One 2012;7:e40378.

Ghosh S, Spagnoli GC, Martin I, Ploegert S, Demougin P, Heberer M, et al. Three-dimensional culture of melanoma cells profoundly affects gene expression profile: a high density oligonucleotide array study. J Cell Physiol 2005;204:522–31.

Gray-Shopfer V, Wellbrock C, Marias R. Melanoma biology and new targeted therapy. Nature 2007;445:851–7.

Griffith LG, Swarz MA. Capturing complex 3D tissue physiology in vitro. Nat Rev Mol Cell Biol 2006;7:211–24.

Heilmann S, Ratnakumar K, Langdon EM, Kansler ER, Kim IS, Campbell NR, et al. A quantitative system for studying metastasis using transparent zebrafish. Cancer Res 2015;75:4272–82.

Kaufman CK, Mosimann C, Fan ZP, Yang S, Thomas A, Ablain J, et al. A zebrafish melanoma model reveals emergence of neural crest identity during melanoma initiation. Science 2016;351:aad2197.

Khwaja F, Allen J, Lynch J, Andrews P, Djakiew D. Ibuprofen inhibits survival of bladder cancer cells by induced expression of the p75NTR tumor suppressor protein. Cancer Res 2004;64:6207–13.

Kraemer BR, Snow JP, Vollbrecht P, Pathak A, Valentine WM, Deutch AY, et al. A role for the p75 neurotrophin receptor in axonal degeneration and apoptosis induced by oxidative stress. J Biol Chem 2014;289:21205–16.

Kruger GM, Mosher JT, Bixby S, Joseph N, Iwashita T, Morrison SJ, et al. Neural crest stem cells persist in the adult gut but undergo changes in self-renewal, neuronal subtype potential, and factor responsiveness. Neuron 2002;35:657–69.

Liu YR, Sun B, Zhao XL, Gu Q, Liu ZY, Dong XY, et al. Basal caspase-3 activity promotes migration, invasion, and vasculogenic mimicry formation of melanoma cells. Melanoma Res 2013;23:245–53.

Marchetti D, Parikh N, Sudol M, Gallick GE. Stimulation of the protein tyrosine kinase c-Yes but not c-Src by neurotrophins in human brain-metastatic melanoma cells. Oncogene 1998;16:3253–60.

Marconi A, Borroni RG, Truzzi F, Longo C, Pistoni F, Pellacani G, et al. Hypoxia-Inducible Factor-1α and CD271 inversely correlate with melanoma invasiveness. Exp Dermatol 2015;5:396–8.

Menon DR, Das S, Krepler C, Vultur A, Rinner B, Schauer S, et al. A stress-induced early innate response causes multidrug tolerance in melanoma. Oncogene 2015;34:4545.

Qian F, Vaux DL, Weissman IL. Expression of the integrin alpha 4 beta 1 on melanoma cells can inhibit the invasive stage of metastasis formation. Cell 1994;77:335–47.

Quintana E, Shackleton M, Foster HR, Fullen DR, Sabel MS, Johnson TM, et al. Phenotypic heterogeneity among tumorigenic melanoma cells from patients that is reversible and not hierarchically organized. Cancer Cell 2010;18:510–23.

Ramgolam K, Lauriol J, Lalou C, Lauden L, Michel L, de la Grange P, et al. Melanoma spheroids grown under neural crest cell conditions are highly plastic migratory/invasive tumor cells endowed with immunomodulator function. PLoS One 2011;6:e18784.

Selimovic D, Sprenger A, Hannig M, Haïkel Y, Hassan M. Apoptosis related protein-1 triggers melanoma cell death via interaction with the juxtamembrane region of p75 neurotrophin receptor. J Cell Mol Med 2012;6:349–61.

Shirley SH, Greene VR, Duncan LM, Torres Cabala CA, Grimm EA, Kusewitt DF. Slug expression during melanoma progression. Am J Pathol 2012;180:2479–89.

Tiberio R, Marconi A, Fila C, Fumelli C, Pignatti M, Krajewski S, et al. Keratinocytes enriched for stem cells are protected from anoikis via an integrin signaling pathway in a Bcl-2 dependent manner. FEBS Lett 2002;524:139–44.

Truzzi F, Marconi A, Atzei P, Panza MC, Lotti R, Dallaglio K, et al. p75 neurotrophin receptor mediates apoptosis in transit-amplifying cells and its overexpression restores cell death in psoriatic keratinocytes. Cell Death Differ 2011;18:948–58.

Truzzi F, Marconi A, Lotti R, Dallaglio K, French LE, Hempstead BL, et al. Neurotrophins and their receptors stimulate melanoma cell proliferation and migration. J Invest Dermatol 2008;128:2031–40.

Vörsmann H, Groeber F, Walles H, Busch S, Beissert S, Walczak H, et al. Development of a human three-dimensional organotypic skin-melanoma spheroid model for in vitro drug testing. Cell Death Dis 2013;4:e719.

White R, Rose K, Zon L. Zebrafish cancer: the state of the art and the path forward. Nat Rev Cancer 2013;13:624–36.